tributors to this zero-point energy difference are the isotopically sensitive umbrella mode and two rocking modes of the methyl groups which are much larger in a covalently bound methyl (in acetone) than in the free methyl moiety.

Input Parameters. The frequencies used to model the transition states in the RRKM calculations of the secondary isotope effect for the stepwise mechanism are listed in Table III. Transition state A and B correspond to CD_3 and CH_3 cleavage, respectively. The input data for the calculation of the absolute rate constants for the first step of the stepwise mechanism (cleavage to the intermediate ion-molecule complex) are given in Table IV.

Registry No. *t*-BuO$^-$, 16331-65-0; D_2, 7782-39-0; CD_3I, 865-50-9; Me_2CO, 67-64-1; MeBr, 74-83-9; $(CD_3)_2CO$, 666-52-4; *t*-BuOSiMe$_3$, 13058-24-7; Me_3SiCl, 75-77-4; $Me_3SiNHAc$, 13435-12-6; $CD_3CMe_2OSiMe_3$, 105457-97-4; 2-methyl-2-propanol-*1,1,1-d*$_3$, 33500-15-1; 2-methyl-2-propanol-*1,1,1,3,3,3-d*$_6$, 53853-65-9.

The Mechanism of Directed Second Lithiations: Detection of Short Proton-Lithium Separations by ^{6}Li-^{1}H HOESY

Walter Bauer, Timothy Clark,* and Paul von Ragué Schleyer

Contribution from the Institut für Organische Chemie der Friedrich-Alexander-Universität, Erlangen-Nürnberg, D-8520 Erlangen, Federal Repulic of Germany. *Received July 3, 1986*

Abstract: Mechanistic details of the specific second metalation of 1-lithionaphthalene (**1**) at the 8-(peri) position, which should be typical of this important class of reactions, have been clarified by a combination of experimental (NMR) and theoretical (MNDO) methods. Complete structural assignments of the ^{1}H and ^{13}C NMR spectra for both *n*-butyllithium (BuLi) in THF-d_8 and **1** in C_6D_6 have been obtained from two-dimensional (2D) NMR experiments (COSY, C-H shift correlation). ^{6}Li-^{1}H HOESY (2D-heteronuclear Overhauser spectroscopy) exhibits cross peaks for H(C_1) and H(C_2) in the BuLi tetramer, indicating some of the Li-H distances to be unusually short. Applied to **1**, the same technique reveals a small distance between Li and H(C_2). However, for a 1:1 mixture of methyllithium and **1**, ^{6}Li-^{1}H HOESY reveals a close contact between Li and H(C_8) (periposition). MNDO calculations indicate that the 2-position of **1** dimer exhibits the shortest H···Li distance but that the 8-position in the mixed CH_3Li-**1** aggregate should be activated. This supports the proposed mechanism for the specific second metalation of **1** by BuLi, which involves reaction within a mixed cluster of **1** and the RLi metalation reagent.

The presence of lithium in a molecule often directs further metalation to a specific position.[1] For example, *n*-butyllithium (BuLi) converts 1-lithionaphthalene (**1**) to the 1,8-dilithio derivative (**2**). On the basis of semiempirical MO calculations, we have suggested that C—Li···H bridging in mixed alkyl/aryl lithium clusters may be responsible for specifically activating one C-H bond in the molecule.[1] We now report a combined NMR and MNDO investigation designed to elucidate the structures of the species found in alkyl/aryl lithium reaction mixtures in solution. These are often, but not always, related to crystal structures obtained by X-ray crystallography[2,3] but involve species for which crystalline samples cannot be obtained. We have applied ^{1}H-^{1}H shift correlation (correlated spectroscopy, COSY) and ^{13}C-^{1}H shift correlation spectroscopy[4] to assign completely the spectra of the lithium compounds investigated. The ^{1}H chemical shifts thus obtained form the basis for the application of two-dimensional heteronuclear Overhauser spectroscopy (HOESY)[5] (analogous to the homonuclear NOESY[6] experiment), using ^{6}Li and ^{1}H nuclei. This technique, which has never been applied to ^{6}Li nuclei before, allows the detection of close Li-H contacts. We have suggested such contacts to be responsible for C-H activation. The use of a high-field (9.4 T) spectrometer allows ^{6}Li-^{1}H HOESY experiments to be carried out with natural abundance samples. The results obtained are confirmed and extended by MNDO calculations.

NMR Results

We first describe the results of NMR investigations on *n*-butyllithium, which serve to illustrate the techniques employed, and then on 1-naphthyllithium (**1**).

***n*-Butyllithium (*n*-BuLi).** The nature of *n*-BuLi, the most important organolithium reagent, and the reactivity of its oligomers have been studied by ^{1}H NMR spectroscopy.[7] A dimer-tetramer equilibrium in tetrahydrofuran-d_8 (THF-d_8) solution at low temperatures was established both by ^{1}H[7] and by ^{13}C NMR,[8] and the kinetics were analyzed by NMR line shape analysis.[9] The full ^{13}C NMR assignment for a benzene-d_6 solution at room temperature (involving rapid interchange between aggregates on the NMR time scale) has been described.[10]

In 1.6 M *n*-BuLi in THF-d_8 at -96 °C, the dimer-tetramer equilibrium is shifted toward the tetramer. The one-dimensional ^{1}H NMR spectrum (Figure 1) shows the rotation around at least some of the C-C bonds to be slow on the NMR time scale. The magnetically nonequivalent pairs of α-, β- and γ-protons give rise

(1) This is the third paper in a series on regioselective metalations. (a) Part 1: Neugebauer, W.; Kos, A. J.; Schleyer, P. v. R. *J. Organomet. Chem.* **1982**, *228*, 107. (b) Part 2: Neugebauer, W.; Clark, T.; Schleyer, P. v. R. *Chem. Ber.* **1983**, *116*, 3283. Also see: Bauer, W.; Müller, G.; Pi, R.; Schleyer, P. v. R. *Angew. Chem.*, in press.

(2) Wardell, J. L. In *Comprehensive Organometallic Chemistry*; Wilkinson, G., Stone, F. G. A., Abel, E. W., Eds.; Pergamon: Oxford, 1982; Vol. 1, p 43ff.

(3) Setzer, W. N.; Schleyer, P. v. R. *Adv. Organomet. Chem.* **1985**, *24*, 353. Schleyer, P. v. R. *Pure Appl. Chem.* **1984**, *56*, 151.

(4) Bax, A. *Two Dimensional Nuclear Magnetic Resonance*; D. Reidel: Dordrecht (Holland), 1984. Günther, H. *Angew. Chem., Int. Ed. Engl.* **1983**, *22*, 350.

(5) Yu, C.; Levy, G. C. *J. Am. Chem. Soc.* **1984**, *106*, 6533.

(6) Jeener, J.; Meier, B. H.; Bachmann, P.; Ernst, R. R. *J. Chem. Phys.* **1979**, *71*, 4546. Meier, B. H.; Ernst, R. R. *J. Am. Chem. Soc.* **1979**, *101*, 6441.

(7) McGarrity, J. F.; Ogle, C. A. *J. Am. Chem. Soc.* **1985**, *107*, 1805. McGarrity, J. F.; Ogle, C. A.; Brich, Z.; Loosli, H.-R. *J. Am. Chem. Soc.* **1985**, *107*, 1810.

(8) Seebach, D.; Hässig, R.; Gabriel, J. *Helv. Chim. Acta* **1983**, *66*, 308.

(9) Heinzer, J.; Oth, J. F. M.; Seebach, D. *Helv. Chim. Acta.* **1985**, *68*, 1848.

(10) Bywater, S.; Lachance, P.; Worsfold, D. J. *J. Phys. Chem.* **1975**, *79*, 2148.

0002-7863/87/1509-0970$01.50/0

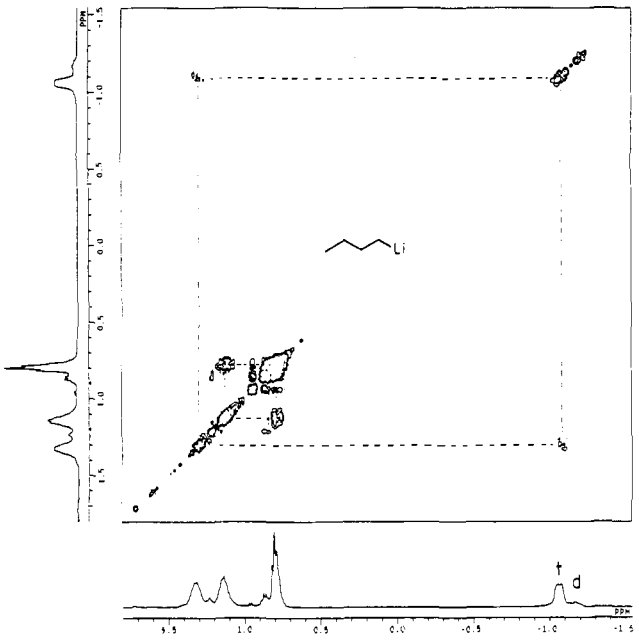

Figure 1. COSY-45 spectrum (400 MHz) of *n*-BuLi in THF-d_8 at −96 °C: d = dimer, t = tetramer.

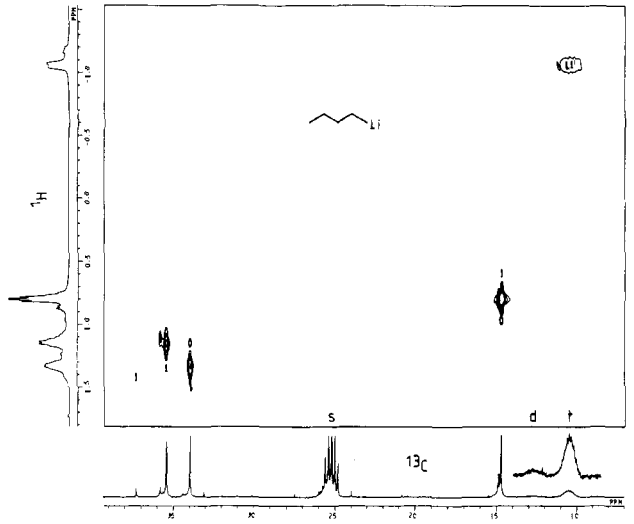

Figure 2. C–H shift correlated spectrum (contour plot) of BuLi; ~2 M in THF-d_8, −96 °C. The contours of the cross peak between H-1 and C-1 (upper right) were taken at a lower level than those of the remaining signals: t = tetramer, d = dimer, s = solvent.

to complex, unresolved peaks. Of the two signal groups at about −1.1 ppm the one at lower field must be assigned to the tetramer because its intensity decreases on dilution. On warming to −30 °C, both the exchange between dimer and tetramer and C–C bond rotation become rapid on the NMR time scale, and well-resolved signal groups appear with a shape similar to that observed for *n*-butylsodium[11] and *n*-butylpotassium[12] in THF-d_8 at −75 and −60 °C, respectively.

The COSY spectrum of *n*-BuLi (Figure 1) allows the unambiguous assignment of the ^{1}H signals of the tetramer: the α-CH_2Li protons at −1.03 ppm exhibit a cross peak with the low field signal group at 1.35 ppm, which thus are due to the β-protons. On the other hand, the methyl signal at 0.82 ppm shares a cross peak with the γ-protons at 1.15 ppm.

The one-dimensional ^{13}C NMR spectrum (Figure 2, bottom) shows four strong signals of the *n*-BuLi tetramer. In a sample

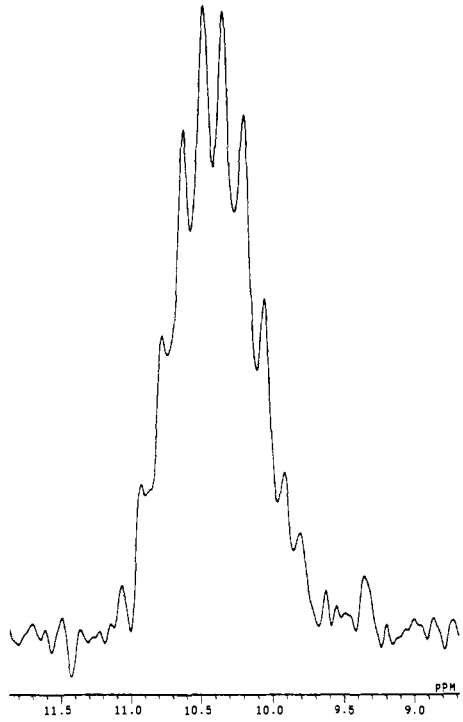

Figure 3. *n*-BuLi, expanded region of C-1 of the tetramer, taken from the one-dimensional ^{13}C spectrum in Figure 2 with resolution enhancement.

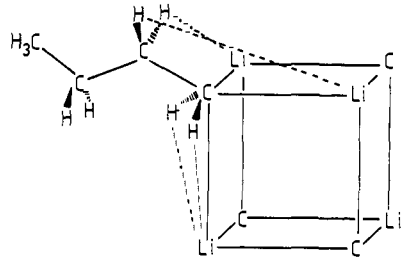

Figure 4. *n*-BuLi tetramer model with indicated short (< ca. 3.5 Å) proton–lithium distances. The conformation of the *n*-butyl group is assumed to be the most favorable energetically.

enriched with ^{6}Li and ^{13}C in the α-position, Seebach et al.[8] assigned the broad ^{13}C NMR signal at 12.5 ppm to the *n*-BuLi dimer because of the 5-line splitting. However, the higher field signal at 10.5 ppm remained unresolved in their experiments. Figure 3 shows the 10.5-ppm signal obtained under our recording conditions. After application of resolution enhancement (Lorentzian to Gaussian transformation),[4] a clear splitting into 10 lines with J = 14.6 Hz is observed. This results from coupling of a ^{13}C nucleus with three ^{7}Li isotopes ($I = {}^3/_2$). These isotopes must be the three equally distant neighbors to ^{13}C in a C_4Li_4-cubic arrangement (cf. Figure 4), whereas coupling to the remote Li atom is not observed.[8] The magnitude of the ^{13}C–^{7}Li coupling is equal to that observed by McKeever and Waack[13] for *n*-BuLi in ether at −70 °C. The Seebach model[8] of a "static" *n*-BuLi tetramer is therefore confirmed. Evidently, the data given in ref 13 describe the *tetramer*. The calculated coupling constant $J_{^{13}C-^6Li}$ for a pure ^{6}Li-containing tetramer would be 5.5 Hz, the value expected for alkyllithium tetramers.[14]

Short proton–proton distances (less than ca. 4 Å) are detected by the nuclear Overhauser effect (NOE) difference spectra[15,16]

(11) Schade, C.; Bauer, W.; Schleyer, P. v. R. *J. Organomet. Chem.* **1985**, *295*, C25.
(12) Pi, R.; Bauer, W.; Brix, B.; Schade, C.; Schleyer, P. v. R. *J. Organomet. Chem.* **1986**, *306*, C1.
(13) McKeever, L. D.; Waack, R. *Chem. Commun.* **1969**, 750.
(14) The coupling constant is proportional to the magnetogyric ratios of the coupled nuclei; $\gamma(^6Li)/\gamma(^7Li) = 0.379$.
(15) Noggle, J. H.; Schirmer, R. E. *The Nuclear Overhauser Effect*; Academic: New York, 1971.
(16) Benn, R.; Rufińska, A.; Schroth, G. *J. Organomet. Chem.* **1981**, *217*, 91.

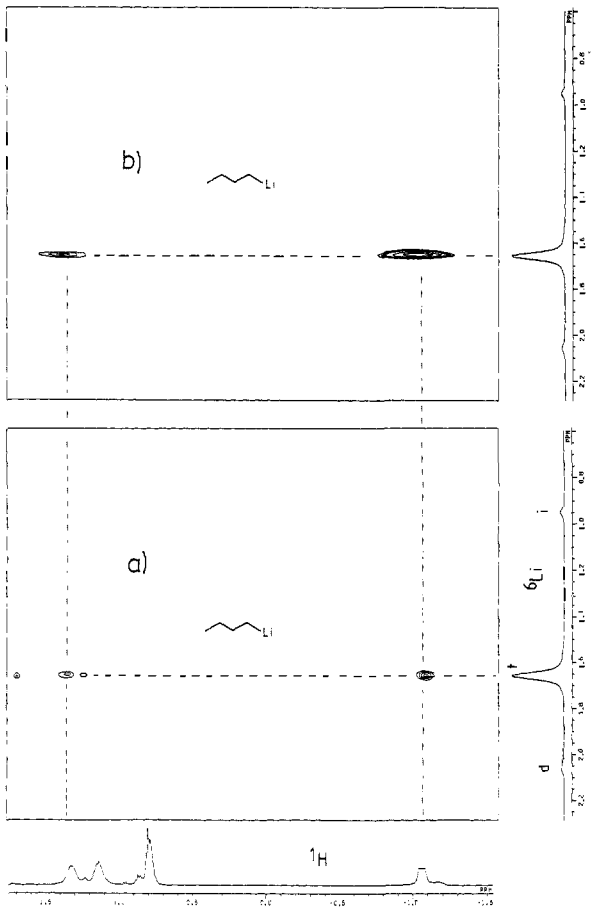

Figure 5. ^{6}Li–^{1}H 2D HOESY plot of *n*-BuLi (natural abundance ^{6}Li), 1.6 M in THF-d_8 at −96 °C: (a) mixing time τ = 1.2 s, 64 increments in t_1 (mesuring time 4 h); (b) mixing time τ = 1.8 s, 9 increments in t_1 (measuring time 0.5 h); t = tetramer, d = dimer, i = impurity.

or by the two-dimensional NOESY sequence.[6] Dipole–dipole relaxation through space and not scalar coupling through bonds is responsible for this phenomenon.

A 2D NMR method for detecting nearby *heternuclei*, e.g., ^{13}C and ^{1}H, heteronuclear Overhauser effect spectroscopy (HOESY),[5] employs the pulse sequence: 90°(^{1}H)–t_1/2–180°(Het)–t_1/2–90°(^{1}H)–mixing time–90°(Het)–FID/^{1}H–BB–decoupling. We now report the application of the 2D HOESY sequence to the location of nearby ^{6}Li nuclei (in natural abundance) and protons in organolithium compounds.

Lithium consists of the isotopes ^{6}Li (7.4%, spin I = 1) and ^{7}Li (92.6%, spin I = $^3/_2$). Because of its small quadrupole moment, ^{6}Li behaves almost like a spin $^1/_2$ nucleus, in that sense that sharp resonance lines (below 1 Hz in certain instances) are observed[17] due to the long spin–lattice relaxation times (T_1). For *n*-BuLi in hexane (2 M, 28 °C), a T_1 value of 19.8 s was found by Wehrli.[17] The same author describes an ^{6}Li–^{1}H nuclear overhauser enhancement factor $\eta_{^6\mathrm{Li}\{^1\mathrm{H}\}}$ = 1.19 for *n*-BuLi, corresponding to 35% intramolecular ^{6}Li–^{1}H dipole contribution to the ^{6}Li relaxation rate (theoretical maximum value $\eta_{^6\mathrm{Li}\{^1\mathrm{H}\}_{max}} = \gamma_{^1\mathrm{H}}/2\gamma_{^6\mathrm{Li}}$ = 3.40). Therefore, the ^{6}Li isotope, although a spin I = 1 nucleus, should be suited for the HOESY sequence.

As a first test we applied the ^{6}Li–^{1}H HOESY experiment to *n*-BuLi (natural isotope abundance) in THF-d_8. Inspection of a model of the *n*-BuLi tetramer reveals short Li–H distances between the α-CH_2 protons and somewhat larger distances between the β-CH_2 protons and the Li nuclei, respectively, in the central C_4Li_4 cube (Figure 4).

Although several conformations of the *n*-butyl group may be present, the mean distance between the α-CH_2 protons and lithium is smaller than that of the β-CH_2 protons and lithium. The ^{6}Li–^{1}H HOESY spectrum confirms this expectation: large and small cross peaks between the ^{6}Li signal of the *n*-BuLi tetramer and the α- and β-CH_2 protons, respectively, are observed (Figure 5).

As can be seen from Figure 5b, even a short 2D experiment with only nine increments and consequently poor resolution in the f_1 dimension produces intensive cross peaks. The intensity of the cross peaks depends on the length of the mixing time. As was deduced from further experiments, a mixing time of 2.0 ± 0.6 s gives the best results.

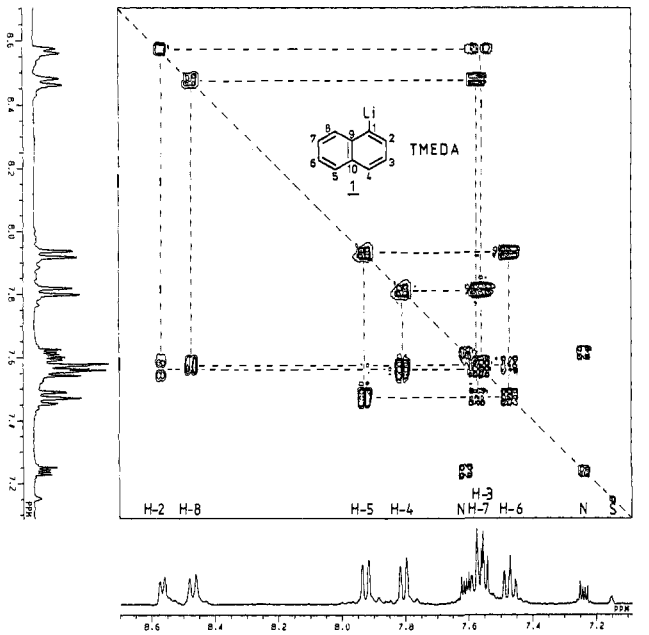

Figure 6. COSY plot of 1-lithionaphthalene (**1**)·TMEDA in C_6D_6 at +25 °C. Only the aromatic signals are shown. For the assignments given see Figure 11a. N = naphthalene, S = solvent.

Scheme I

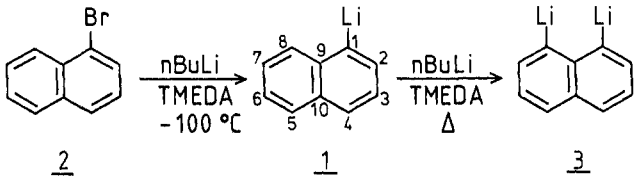

1-Lithionaphthalene (1). The monolithio compound **1**·TMEDA was isolated as a black-green precipitate.[1] Its ^{1}H NMR spectrum in C_6D_6 solution (Figures 6 and 11) at 400 MHz can be analyzed according to first-order rules. The prominent low-field doublet at δ 8.57 is assigned to H-2 as the vicinal coupling constant $^3J_{H\text{-}2/H\text{-}3}$ is smaller (5.8 Hz) than that in the unsubstituted hydrocarbon (6.85 Hz).[18] This difference is well-known in aromatic compounds with electropositive substituents.[19] However, this contradicts an earlier assignment for the proton spectrum of **1** in diethyl ether.[20]

The COSY experiment on **1**·TMEDA confirms unambiguously our assignment of the proton signals (Figure 6): the doublet at 8.57 ppm shares a cross peak with the double doublet at 7.56 ppm, which in turn is coupled to the doublet at 7.81 ppm. These three signal groups must arise from the "metalated half" H-2, H-3, and H-4 in **1**. On the other hand, the doublet at 8.47 ppm has a cross peak with the "triplet" at 7.57 ppm. This signal is coupled with the 7.47 ppm "triplet" which in turn corresponds to the doublet at 7.93 ppm. This signal group must be the unsubstituted ring, H-5, H-6, H-7, and H-8 in **1**.

With the aid of the assigned ^{1}H spectrum of **1**·TMEDA, the corresponding ^{13}C spectrum can be analyzed completely by means of the C–H shift correlated spectrum. In Figure 7a the delays in the pulse sequence[21] are set for a coupling constant $^1J_{C\text{-}H}$ =

(17) Wehrli, F. W. *Org. Mag. Reson.* **1978**, *11*, 106.

(18) Pawliczek, J. B.; Günther, H. *Tetrahedron* **1970**, *26*, 1755.
(19) Castellano, S.; Sun, C. *J. Am. Chem. Soc.* **1966**, *88*, 4741.
(20) Böll, W. A. *Tetrahedron Lett.* **1968**, 2595.

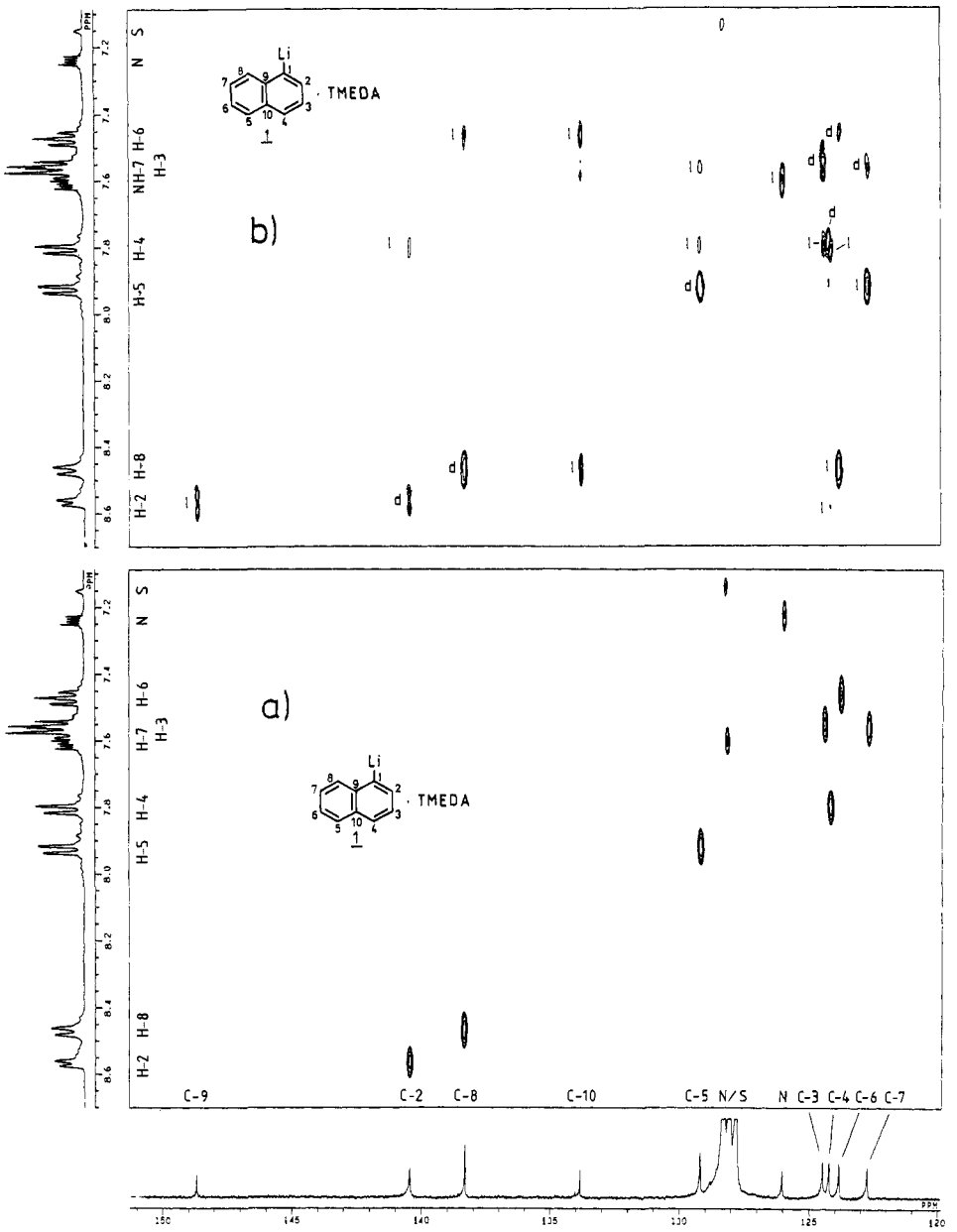

Figure 7. C–H shift correlated spectra of 1-lithionaphthalene (**1**)·TMEDA in C_6D_6 at +23 °C. The signal of C-1 and the carbon and proton signals of TMEDA are omitted: (a) delays optimized for direct C–H couplings; (b) delays optimized for long-range couplings. N = naphthalene, S = solvent, d = cross peak from direct coupling, l = cross peak from long-range coupling.

160 Hz. The assignments of the tertiary carbons in **1** are evident from the spectra.

The lithiated carbon C-1 in **1** is not included in Figure 7 and resonates at 195.0 ppm. The reasons for this unexpected downfield shift (cf. phenyllithium: $\delta_{C\text{-}1}$ = 188.9 ppm)[8] have been discussed elsewhere.[8] In naphthalene derivatives with electropositive substituents in the 1-position, the quaternary carbon C-9 resonates at lower field than C-10 (e.g., 1-(trimethylsilyl)naphthalene: $\delta_{C\text{-}9}$ = 137.4 ppm, $\delta_{C\text{-}10}$ = 133.8 ppm;[21] naphthalene: $\delta_{C\text{-}9}$ = 133.7 ppm). Therefore, the carbon signal at δ = 148.7 ppm in Figure 7 can be assigned to C-9, whereas C-10 appears at δ = 133.8 ppm. An independent proof for the assignment of the quaternary carbons in **1** is given by a C–H shift correlated spectrum with delays optimized for long-range couplings (Figure 7b): C-9 and C-10 each exhibit $^3J_{C\text{–}H}$ couplings to H-2 and H-8, respectively.

Of the remaining carbon atoms, C-2 and C-8 are shifted remarkably strongly downfield relative to naphthalene ($\Delta\delta$ = 14.8 and 10.6 ppm, respectively). The same tendency is observed in group IVB substituted 1-naphthyl systems.[22] At least for silicon, this effect has been ascribed to π-electron withdrawal by the substituent.[22]

According to Scheme I the introduction of a second lithium atom in **1** proceeds exclusively in the peri-(8) position. Regiospecific second metalation has been observed in several more examples.[1,3] On the basis of reasons of Coulombic interactions, symmetrically (**4**, **5**) or unsymmetrically (**6**) double lithium bridged or unsymmetrically double lithium substituted (**7**)[3,23] species may arise. The experimentally found positions of the second lithiations coincide with predictions from semiempirical (MNDO) calculations: the activation of the hydrogen to be replaced next by lithium is indicated by a comparatively large LUMO coefficient and a reduced C–H bond order.[24] As stated

(21) Freeman, R.; Morris, G. A. *Chem. Commun.* **1978**, 684.

(22) Bullpitt, M.; Kitching, W.; Adcock, W.; Doddrell, D. *J. Organomet. Chem.* **1976**, *116*, 161.

(23) Neugebauer, W.; Kos, A. J.; Schleyer, P. v. R. *J. Organomet. Chem.* **1982**, *228*, 107. Schubert, U.; Neugebauer, W.; Schleyer, P. v. R. *Chem. Commun.* **1982**, 448. Schleyer, P. v. R.; Kos, A. J.; Wilhelm, D.; Clark, T.; Boche, G.; Decher, G.; Etzrodt, H.; Dietrich, H.; Mahdi, W. *Chem. Commun.* **1984**, 1495. Streitwieser, A., Jr.; Swanson, J. T. *J. Am. Chem. Soc.* **1983**, *105*, 2502.

(24) Schleyer, P. v. R. *Pure Appl. Chem.* **1983**, *55*, 355.

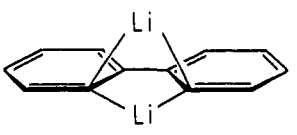

4

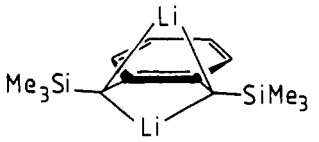

5

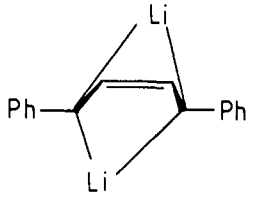

6

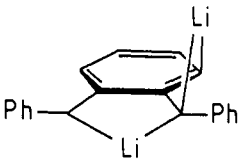

7

above, the ^{6}Li–^{1}H HOESY experiment can serve as a probe for examining this activation by the detection of small ^{6}Li–^{1}H distances. Therefore, we applied the 2D HOESY experiment to 1-lithionaphthalene (**1**) with natural isotope abundance (Figure 8).

Two cross peaks are observed; one is due to the N–CH_3 signal of TMEDA, i.e., the ligand must be tightly bound to the cation with the methyl group closer to lithium than the methylene group. This is confirmed by molecular models. Clearly, the second cross peak in Figure 8 does *not* correlate to the peri-hydrogen in **1**, but it indicates close contact between lithium and H-2. Considering the above arguments, H-2 rather than H-8 should be "activated" toward second metalation.

MNDO Results and Discussion

The results of the HOESY experiment just described are confirmed by MNDO calculations on **1**. Low-temperature ^{13}C spectra on the ^{6}Li-labeled compounds would allow direct observation of the degree of aggregation,[25] but in this case, only natural abundance ^{6}Li/^{7}Li samples were available. However, 1-lithionaphthalene has been found to be dimeric by ebullioscopic measurements;[26] phenyllithium is a dimer in the solid state and in solution.[27] Figure 9 shows the MNDO optimized geometry of the 1-lithionaphthalene dimer in C_i symmetry. For symmetry reasons, four different pairs of distances between the Li atoms and H-2,2′ and H-8,8′ result. Clearly, the mean Li–H-8,8′ value (3.26 Å) is larger than that for Li–H-2,2′ (2.89 Å). The activation of the "wrong" H-2 in **1** by Li can also be seen from the LUMO coefficients (H-2,2′ −0.00242, H-8,8′ 0.00026) and from the C–H bond orders (C-2,2′/H-2,2′ 0.936, C-8,8′/H-8,8′ 0.953).

How then can the exclusive second metalation in the 8-position be explained? When **1**·TMEDA is treated with a second equivalent of *n*-BuLi at room temperature, an exothermic process occurs.[1] However, as prolongued heating is needed for the complete introduction of the second metal atom, this initial process obviously cannot be the metalation reaction but indicates the formation of a complex between **1** and *n*-BuLi. Therefore, this initial *complex*, rather than **1** or its dimer, has to be considered in order to explain the observed regiospecific second metalation. For both the calculations and the NMR experiments, we employed methyllithium (MeLi) rather than *n*-BuLi.

The existence of analogous mixed dimers was demonstrated, e.g., for the lithiophenyl acetylene–*n*-BuLi complex **4**.[28] The

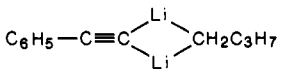

4

MNDO results for a mixed **1**·CH_3Li complex are shown in Figure 10. According to MNDO calculations, the *8-position* in **1**·CH_3Li is now activated; thus, the mean bond length Li–H-8 (2.99 Å) is shorter than the mean distance Li–H-2 (3.10 Å); the LUMO coefficient of H-8 is larger than that of H-2; the bond order C-8/H-8 is smaller than that of C-2/H-2.

The ^{1}H NMR spectrum of the **1**·CH_3Li complex shows a drastic effect on the chemical shifts of H-2 and H-8, which interchange their positions: the doublet with the lower coupling constant (H-2) now appears at higher field than H-8 (Figure 11).

The 2D HOESY spectrum of the **2**·CH_3Li·3TMEDA complex, when recorded in C_6D_6 at room temperature, shows only cross peaks to the TMEDA–N–CH_3 and the CH_3Li protons. No cross peaks to the aromatic protons could be detected under these recording conditions. As the nuclear Overhauser effect is known to change its magnitude and sign with temperature,[15] a small or zero NOE might be the reason for the missing cross peak. However, the same sample when stripped of the C_6D_6 solvent and replaced with toluene-d_8 gave a HOESY spectrum (Figure 12) with an additional cross peak in the aromatic region when measured at −85 °C. Clearly, this peak *now* involves the H-8 proton replaced during the second metalation.

The observation of H-8 activation in **1**·CH_3Li coincides nicely with the experimental results. Thus, ^{6}Li–^{1}H HOESY is a new tool for investigating structures of organolithium compounds. Information can be obtained about the Li cation location in solution, under circumstances relevant to synthetic applications and in molecules whose structure cannot be determined by X-ray crystallography. Furthermore, our results once again confirm the usefulness of MNDO calculations for the study of the structures and reactivities of organolithium compounds.

Experimental Section

Instrumental. NMR spectra were recorded on a JEOL JNM-GX 400 spectrometer. Measuring frequencies were 400 MHz (^{1}H), 100.6 MHz (^{13}C), and 58.8 MHz (^{6}Li). Quadrature detection was carried out in both dimensions for 2D spectra. Chemical shifts are reported in ppm downfield from Me_4Si. Carbon signals and residual proton signals of the deuterated solvents were used as internal reference. THF-d_8: ^{1}H 3.58 ppm (α-proton), ^{13}C 67.4 ppm (α-carbon). C_6D_6: ^{1}H 7.15 ppm, ^{13}C 128.0 ppm. Toluene-d_8: ^{1}H 2.03 ppm (methyl group), ^{13}C 20.4 ppm (methyl group). ^{6}Li chemical shifts are relative to 1 M LiBr (anhydrous) in THF/THF-d_8 5:1 (v/v) = 0 ppm. The reference measurements were carried out in independent runs with use of THF-d_8 lock at the appropriate temperatures. No susceptibility corrections were made for either C_6D_6 or toluene-d_8. The ^{13}C- and ^{6}Li-90°-pulse lengths were calibrated in the usual manner,[29] and the ^{1}H-90°-pulse length was adjusted via the INEPT sequence.[30]

Preparation of NMR Samples. *n*-Butyllithium (BuLi). A 5-mm NMR tube was fitted with a serum cap, flame dried in vacuo and cooled under argon with a hypodermic needle. A BuLi/hexane solution (0.7 mL, 1.6 M) was added by syringe. The solvent was stripped off at room temperature in vacuo and replaced at −78 °C by 0.6 mL of THF-d_8 (dried over Na/Pb alloy). The tube was sealed thoroughly with parafilm and stored at −78 °C. Spectral data: ^{1}H NMR (THF-d_8, −96 °C) 1.43–1.27 (m, H-2 tetramer/dimer), 1.25–1.05 (m, H-3 tetramer/dimer), 0.90–0.75 (2 t, 7.1 Hz, H-4 tetramer/dimer) −1.00 to −1.06 (m, H-1 tetramer) −1.10 to −1.18 (m, H-1 dimer); ^{13}C NMR (THF-d_8, −96 °C) 35.4 (C-3), 33.9 (C-2), 14.7 (C-4), 10.5 (C-1).

1-Lithionaphthalene (1·TMEDA). Prepared from 1-bromonaphthalene[1] 158 mg (0.63 mmol) of dark green powdery **1**·TMEDA was placed in a flame-dried (see above) 10-mm NMR tube under argon in a glovebox. C_6D_6 (2.0 mL, dried over Na/Pb alloy) was added via syringe at room temperature, and the tube was sealed with Parafilm.

Spectral data: ^{1}H NMR (C_6D_6, +22 °C) 8.57 (d, 5.8 Hz, H-2), 8.47 (d, 8.0 Hz, H-8), 7.93 (d, 8.0 Hz, H-5), 7.81 (d, 8.0 Hz, H-4), 7.57 (ddd, 8.0 , 6.8, 1.2 Hz, H-7), 7.56 (dd, 8.0, 5.8 Hz, H-3), 7.47 (ddd, 8.0, 6.8, 1.2 Hz, H-6), 1.65 (s, N-CH_3), 1.54 (s, N-CH_2); ^{13}C NMR (C_6D_6, +24

(25) Fraenkel, G.; Henrichs, M.; Hewitt, J. M.; Su, B. M.; Geckle, M. J. *J. Am. Chem. Soc.* **1980**, *102*, 3345. Fraenkel, G.; Hsu, H.; Su, B. M. In *Lithium: Current Applications in Science, Medicine and Technology*; Bach, R. O., Ed.; Wiley: New York, 1985; p 273.

(26) Rodionov, A. N.; Shigorin, D. N.; Talalaeva, T. V.; Tsareva, G. V.; Kocheshkov, K. A. *Zh. Fiz. Khim.* **1966**, *40*, 2265; *Chem. Abstr.* **1967**, *66*, 28268e.

(27) Thoennes, D.; Weiss, E. *Chem. Ber.* **1978**, *111*, 3157. Bauer, W.; Seebach, D. *Helv. Chim. Acta* **1984**, *67*, 1972. Some monomer was found in THF at −108 °C by cryoscopy.

(28) Hässig, R.; Seebach, D. *Helv. Chim. Acta* **1983**, *66*, 2269.

(29) Martin, M. L.; Martin, G. J.; Delpuech, J.-J. *Practical NMR Spectroscopy*; Heyden: London, 1980; p 267.

(30) Morris, G. A.; Freeman, R. *J. Am. Chem. Soc.* **1979**, *101*, 760.

Table I. Experimental Conditions of 2D NMR Spectra

sample	experiment	tube diameter (mm)	solvent	temp (°C)	freq range [f_1 (Hz); f_2 (Hz)]	scans per increment	recorded increments in t_1	filtering function[a] (t_1; t_2)	data matrix size (t_1; t_2)
n-BuLi	COSY-45	5	THF-d_8	−96	1337; 1337	8	256	4; 4	256; 1024
	C–H shift correlation	5	THF-d_8	−96	1337; 3160	32	112	2; 2	256; 2048
	^{6}Li–^{1}H HOESY	5	THF-d_8	−96	1337; 100	16	64	2; 1	256; 512
1·TMEDA	COSY	10	C_6D_6	+21	645; 645	16	64	3; 3	256; 1024
	C–H shift[b] correlation	10	C_6D_6	+21	645; 3160	32	64	2; 2	128; 2048
	^{6}Li–^{1}H HOESY	10	C_6D_6	+20	3232; 100	32	46	2; 1	256; 512
1·CH_3Li·3TMEDA	^{6}Li–^{1}H HOESY	10	toluene-d_8	−85	4566; 200	16	64	2; 1	256; 512

[a] 1 = exponential line broadening; 2 = Lorentzian to Gaussian transformation; 3 = sine bell; 4 = squared sine bell. [b] Direct couplings; Δ_1 = 3.14 ms, Δ_2 = 1.57 ms. Long-range couplings: $\Delta_1 = \Delta_2$ = 37 ms.

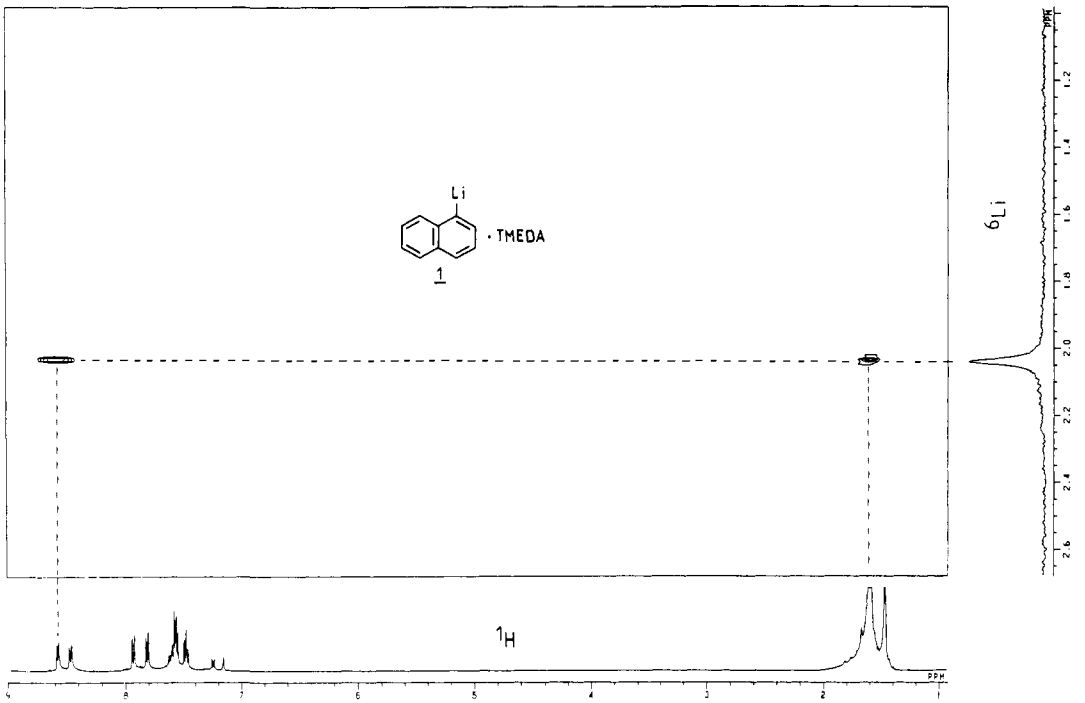

Figure 8. ^{6}Li–^{1}H 2D HOESY spectrum of **1**·TMEDA in C_6D_6 at 23 °C; mixing time τ = 2.1 s.

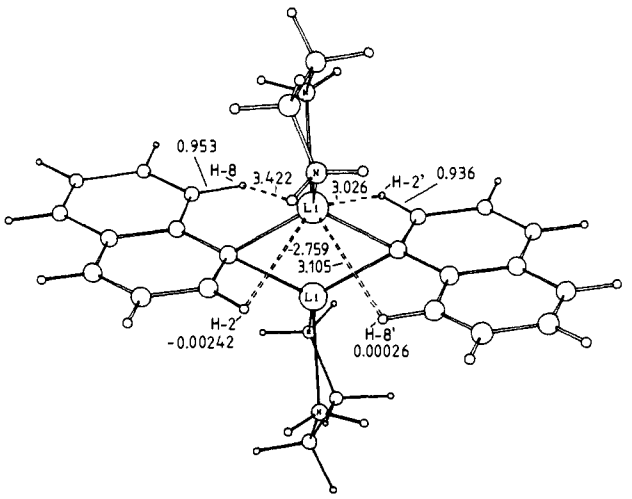

Figure 9. MNDO calculated geometry (C_i symmetry) of the 1-lithionaphthalene dimer with two ethylenediamine ligands; numbers at dashed lines, Li–H distances in Å; numbers at C–H bonds, bond orders; numbers at H atoms, LUMO coefficients.

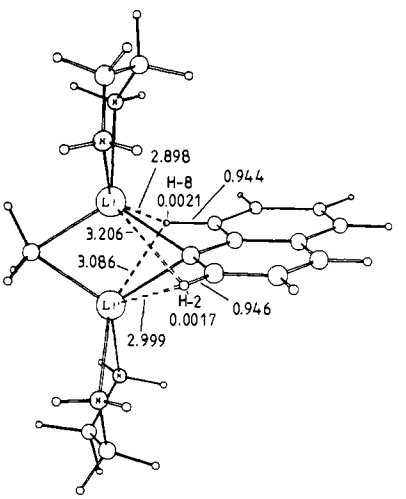

Figure 10. MNDO-optimized geometry of the mixed **1**–CH_3Li dimer with two ethylenediamine ligands; for data cf. Figure 9.

°C) 195.0 (C-1), 148.7 (C-9), 140.4 (C-2), 138.3 (C-8), 133.8 (C-10), 129.2 (C-5), 124.4 (C-3), 124.2 (C-4), 123.8 (C-6), 122.7 (C-7), 57.2 (N-CH_2), 46.4 (N-CH_3).

1-Lithionaphthalene–Methyllithium–3TMEDA Complex. The solvent was removed in vacuo from 3.9 mL (6.24 mmol) of commercial methyllithium in diethyl ether (1.6 M, titrated against diphenylacetic acid).[31] After addition of 5.0 mL of C_6D_6 (dried as described above) the suspension was treated with 2.0 mL (13.2 mmol) of TMEDA (distilled from CaH_2), to give a clear solution. Of this solution 0.7 mL (equal

(31) Kofron, W. G.; Baclawski, L. M. *J. Org. Chem.* **1976**, *41*, 1879.

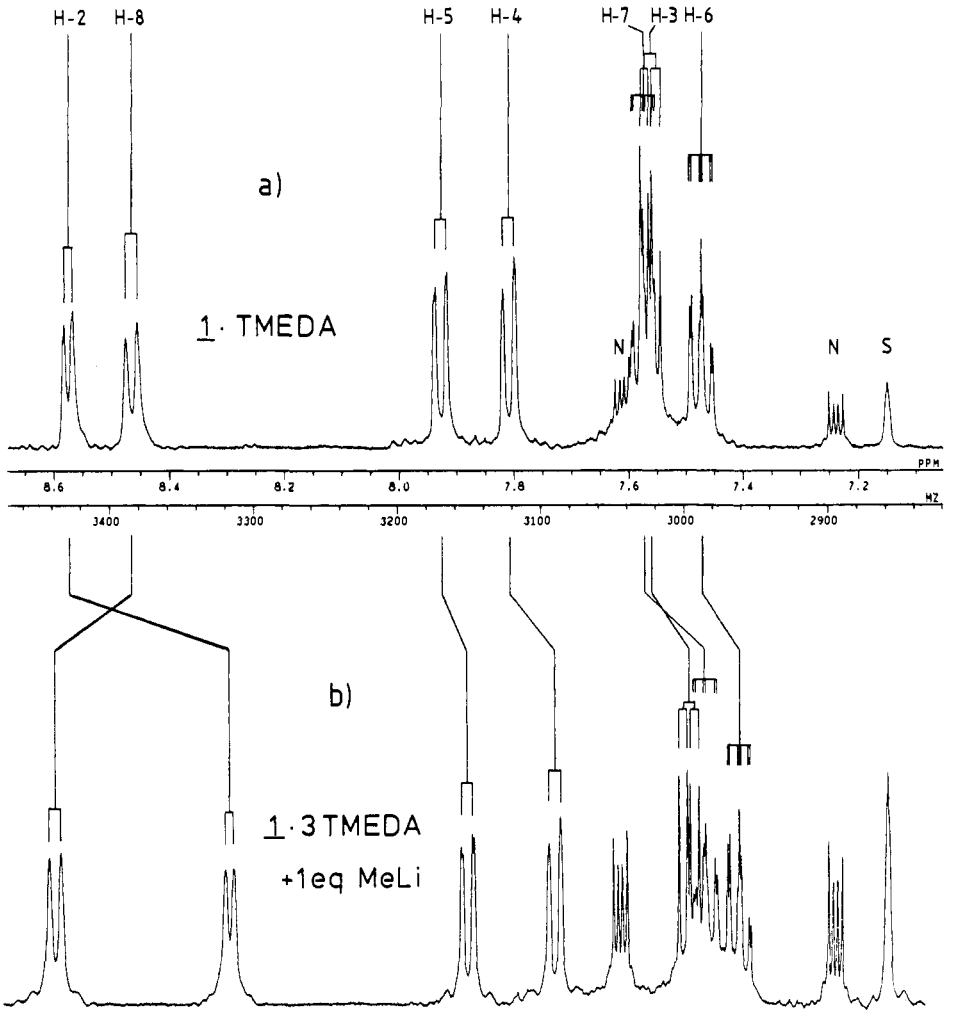

Figure 11. ^{1}H NMR spectra (aromatic region) of **1**·TMEDA (a) and **1**·CH_3Li·3TMEDA (b) in C_6D_6 at 23 °C.

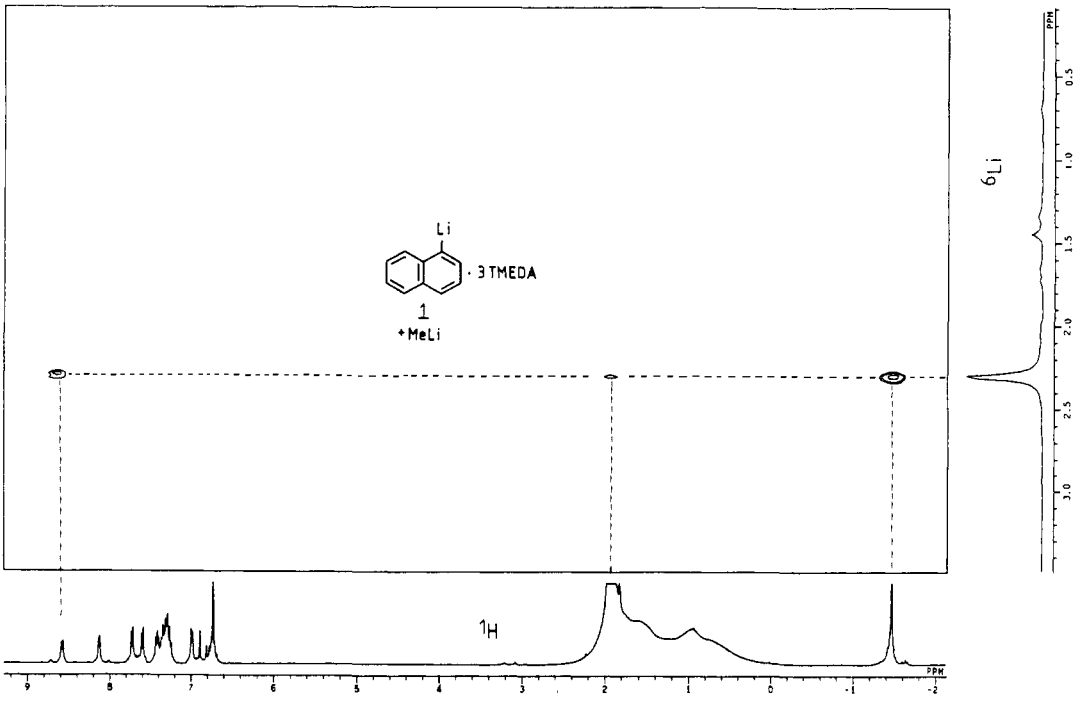

Figure 12. ^{6}Li–^{1}H 2D HOESY spectrum of **1**·CH_3Li·3TMEDA in toluene-d_8, −85 °C, mixing time 1.6 s.

to 0.62 mmol of MeLi) was added by syringe at +5 °C to the contents of the above 10-mm tube. For the ^{6}Li–^{1}H HOESY experiments C_6D_6 was removed in vacuo and replaced by 2.5 mL of toluene-d_8 (dried over Na/Pb alloy).

Spectral data: ^{1}H NMR (C_6D_6, +22 °C) 8.59 (d, 8.0 Hz, H-8), 8.29 (d, 5.6 Hz, H-2), 7.88 (dd, 7.8, 1.5 Hz, H-5), 7.73 (d, 8.0 Hz, H-4), 7.49 (dd, 8.0, 5.6 Hz, H-3), 7.47 (ddd, 8.0, 7.6, 1.5 Hz, H-7), 7.41 (ddd, 7.8, 7.6, 1.4 Hz, H-6), 2.2–0.4 (br, N-CH_3 and N-CH_2), −1.41 (s, CH_3Li);

^{13}C NMR (C_6D_6, +23 °C) 198.9 (C-1), 149.2 (C-9), 141.1 (C-2), 137.5 (C-8), 133.6 (C-10), 124.1, 123.6, 123.5 (C-3, C-4, C-6), 122.3 (C-7), 57.5 (N-CH_2), 46.2 (N-CH_3), -11.7 (CH_3Li).

2D NMR Experiments. The conditions for the 2D NMR measurements on the various samples are summarized in Table I. The pulse sequences were the following: COSY, 90°-t_1-90°/45°-t_2-delay;[32] C-H shift correlation, 90°(^{1}H)-t_1/2-180°(^{13}C)-t_1/2-Δ_1-90°(^{1}H), 90°(^{13}C)-Δ_2-t_2/^{1}H-bb-decoupling-delay;[21] ^{6}Li-^{1}H HOESY, 90°(^{1}H)-t_1/2-180°(^{6}Li)-t_1/2-90°(^{1}H)-τ-90°(^{6}Li)-t_2/^{1}H-bb-decoupling-delay.[5] 2D plots are presented in the absolute value mode. The COSY data matrizes were symmetrized after Fourier transformation. The ^{6}Li-^{1}H HOESY experiments were run with 90° pulse lengths 31 μs (^{6}Li) and 85 μs (^{1}H), respectively, and a pulse delay of 6 to 8 s. For each sample measured, several runs with varying mixing time, τ, were taken. Optimal signal-to-noise ratio was obtained for $\tau \sim 2$ s.

MNDO calculations[33] with parametrization for lithium[34] were carried out on a CYBER 845 and an IBM 4361 computer.

Acknowledgment. This work was supported by the Deutsche Forschungsgemeinschaft and the Fonds der Chemischen Industrie. We thank Dr. M. Feigel for helpful and stimulating discussions.

Registry No. 1-Lithionaphthalene, 14474-59-0.

(32) Bax, A.; Freeman, R. *J. Magn. Reson.* **1981**, *44*, 542.

(33) Dewar, M. J. S.; Thiel, W. *J. Am. Chem. Soc.* **1977**, *99*, 4899, 4907.

(34) Lithium parametrization: Thiel, W.; Clark, T., QCPE Newsletter, submitted. (See the MNDOC Program; Thiel, W. QCPE Program No. 438.)

Theoretical Study of Hydridocobalt Carbonyls

Danko Antolovic and Ernest R. Davidson*

Contribution from the Department of Chemistry, Indiana University, Bloomington, Indiana 47405. *Received June 13, 1986*

Abstract: The molecular geometry and electronic structure of hydridocobalt tri- and tetracarbonyls were investigated, by means of ab initio Hartree-Fock calculations in a Gaussian basis set. Two conformations of the tetracarbonyl were found, both having the d^8, closed-shell electronic configuration. The tricarbonyl complex was found to possess a number of conformations, as well as several low-energy electronic configurations. We examine the geometry, frontier orbitals, and character of chemical bonds of these forms of $HCo(CO)_4$ and $HCo(CO)_3$, with the aim of determining their relevance to the catalytic activity of the compounds.

In this article we endeavor to study the molecular geometry and electronic structure of hydridocobalt tri- and tetracarbonyls. Hydridocobalt tetracarbonyl is a well-known compound, of importance as catalyst in the hydroformylation process.[1] Tricarbonyl, on the other hand, is a largely hypothetical species. It is assumed to be the actual catalyst in the hydroformylation reaction, present in small amounts in the reaction mixture, due to spontaneous decomposition of the tetracarbonyl.

The molecular structure of the tetracarbonyl compound was determined by gas-phase electron diffraction experiments of McNeill and Scholer,[2] who found the molecule to have C_{3v} symmetry and an H-Co bond length of 1.556 Å.

There is only indirect evidence for the existence of $HCo(CO)_3$. Ungvary and Marko[3] have carried out kinetic studies of the decomposition of $HCo(CO)_4$ into dicobalt octacarbonyl and hydrogen under the assumption that the establishment of an $HCo(CO)_4$-$HCo(CO)_3$ equilibrium is the first step in this reaction. Kinetic results are in agreement with this assumption, and the equilibrium constant corresponds to a concentration of $HCo(CO)_3$ equal to roughly 0.3% of the concentration of $HCo(CO)_4$ in *n*-heptane solution.

In a later study, Wermer et al.[4a] have reported evidence for $HCo(CO)_3$ in the IR spectra of the tetracarbonyl in an argon matrix at low temperature. They observed certain weak absorption bands whose intensity grew with irradiation of the sample and decreased in the presence of CO and which they could not assign to any known cobalt carbonyl. Their estimate is that the concentration of $HCo(CO)_3$ amounts to 0.2% of that of $HCo(CO)_4$.

In an independent study of the photolysis of $HCo(CO)_4$ in the argon and carbon monoxide matrices, Sweany[4b] reinterprets the observations made by Wermer et al.[4a] and assigns two of the mentioned IR bands to the species $Co(CO)_4$. This study assigns only one IR band to $HCo(CO)_3$.

To date, there are no experimental results concerning the molecular geometry or the electronic structure of the tricarbonyl compound.

Both of these compounds have been the subject of theoretical investigations involving a range of computational techniques (extended Hückel theory,[5-7] CNDO/2,[8] INDO/1,[9] SCF-LCAO-MO,[8,10] SCF-Xα-SW[11]). All of these studies agree in depicting $HCo(CO)_4$ as a closed-shell, d^8-complex with C_{3v} symmetry. Details of the predicted geometry correspond qualitatively to those found experimentally. For the tricarbonyl compound, on the other hand, there is no such consensus: different computational methods vary on the subject of the relative stability of different conformations of this complex, as well as on the details of its electronic structure.

We find theoretically predicted geometries, as reported in the literature, rather inconclusive. Some optimizations are incomplete;[8,10] in other cases it is not clear whether the reported symmetry is the result of a full geometry optimization or an ad hoc constraint.[6,8] Finally, some semiempirical methods[9,12] have, in the authors' experience, yielded unphysical geometries and should not be relied upon too strongly.

(1) Orchin, M. *Acc. Chem. Res.* **1981**, *14*, 259.
(2) McNeill, E. A.; Scholer, F. R. *J. Am. Chem. Soc.* **1977**, *99*, 6243.
(3) Ungvary, F.; Marko, L. *J. Organomet. Chem.* **1969**, *20*, 205.
(4) (a) Wermer, P.; Ault, B. S.; Orchin, M. *J. Organomet. Chem.* **1978**, *162*, 189. (b) Sweany, R. L. *Inorg. Chem.* **1980**, *19*, 3512.
(5) Pensak, D. A.; McKinney, R. J. *Inorg. Chem.* **1979**, *18*, 3407.
(6) Bellagamba, V.; Ercoli, R.; Gamba, A.; Suffritti, G. B. *J. Organomet. Chem.* **1980**, *190*, 381.
(7) Boudreaux, E. A. *Inorg. Chim. Acta* **1984**, *82*, 183.
(8) Grima, J. Ph.; Choplin, F.; Kaufmann, G. *J. Organomet. Chem.* **1977**, *129*, 221.
(9) Iberle, K. A.; Davidson, E. R., unpublished results.
(10) Fonnesbech, N.; Hjortkjaer, J.; Johansen, H. *Int. J. Quantum Chem.* **1977**, *12*, 95.
(11) Eyermann, C. J.; Chung-Phillips, A. *J. Am. Chem. Soc.* **1984**, *106*, 7437.
(12) Various INDO schemes, as implemented in the program ZINDO, written by M. Zerner.

0002-7863/87/1509-0977$01.50/0